



Article

Temperature Dependence of Platelet Metabolism

Freyr Jóhannsson ^{1,2}, James T. Yurkovich ^{3,4,5} , Steinn Guðmundsson ^{1,6}, Ólafur E. Sigurjónsson ^{7,8} 
and Óttar Rolfsson ^{1,2,*} 

- ¹ Center for Systems Biology, University of Iceland, Sturlugata 8, 102 Reykjavik, Iceland
² School of Health Sciences, Medical Department, University of Iceland, Sturlugata 8, 102 Reykjavik, Iceland
³ Department of Bioengineering, University of California San Diego, La Jolla, CA 92093, USA
⁴ Phenome Health, Seattle, WA 98109, USA
⁵ Center for Phenomic Health, The Buck Institute for Research on Aging, Novato, CA 94945, USA
⁶ Faculty of Industrial Engineering, Mechanical Engineering and Computer Science, University of Iceland, Dunhagi 3, 107 Reykjavik, Iceland
⁷ The Blood Bank, Landspítali-University Hospital, Snorrabraut 60, 101 Reykjavik, Iceland
⁸ School of Science and Engineering, Reykjavik University, Menntavegur 1, 102 Reykjavik, Iceland
* Correspondence: ottarr@hi.is; Tel.: +354-5255854

Abstract: Temperature plays a fundamental role in biology, influencing cellular function, chemical reaction rates, molecular structures, and interactions. While the temperature dependence of many biochemical reactions is well defined in vitro, the effect of temperature on metabolic function at the network level is poorly understood, and it remains an important challenge in optimizing the storage of cells and tissues at lower temperatures. Here, we used time-course metabolomic data and systems biology approaches to characterize the effects of storage temperature on human platelets (PLTs) in a platelet additive solution. We observed that changes to the metabolome with storage time do not simply scale with temperature but instead display complex temperature dependence, with only a small subset of metabolites following an Arrhenius-type relationship. Investigation of PLT energy metabolism through integration with computational modeling revealed that oxidative metabolism is more sensitive to temperature changes than glycolysis. The increased contribution of glycolysis to ATP turnover at lower temperatures indicates a stronger glycolytic phenotype with decreasing storage temperature. More broadly, these results demonstrate that the temperature dependence of the PLT metabolic network is not uniform, suggesting that efforts to improve the health of stored PLTs could be targeted at specific pathways.

Keywords: metabolism; platelet concentrates; temperature dependence; metabolic modeling; systems biology



Citation: Jóhannsson, F.; Yurkovich, J.T.; Guðmundsson, S.; Sigurjónsson, Ó.E.; Rolfsson, Ó. Temperature Dependence of Platelet Metabolism. *Metabolites* **2024**, *14*, 91. <https://doi.org/10.3390/metabo14020091>

Academic Editor: Hunter N. B. Moseley

Received: 30 November 2023
Revised: 16 January 2024
Accepted: 19 January 2024
Published: 26 January 2024



Copyright: © 2024 by the authors. Licensee MDPI, Basel, Switzerland. This article is an open access article distributed under the terms and conditions of the Creative Commons Attribution (CC BY) license (<https://creativecommons.org/licenses/by/4.0/>).

1. Introduction

Temperature affects many enzyme-catalyzed biochemical reactions and biological processes. In the late 19th century, van't Hoff and Arrhenius [1] determined that the rate constant k for a large number of chemical reactions can be expressed as an explicit function of temperature

$$k = Ae^{-\frac{E_a}{RT}}$$

where R is the gas constant, T is absolute temperature, E_a is the activation energy of the reaction, and A is known as the pre-exponential factor of the reaction. While this empirical relationship describes the reaction rate of a single chemical reaction, previous studies have shown that the rate of many other more complex processes—such as the chirping of tree crickets [2], muscle contraction [3], drug shelf life [4], and cellular and whole organism metabolism [5–7]—can be modeled by this equation. The rates of these phenomena all depend, at least partly, on chemical reaction rates. The temperature dependence of the rates of biological processes is expressed in the unitless coefficient Q_{10} , the ratio of reaction

rates occurring at temperatures differing by 10 °C [8]. The empirically derived van't Hoff rule states that the Q_{10} for biological processes is generally between 2 and 3 [8–13], with some notable exceptions [6,8]. It is important to note that Q_{10} depends on the measured temperature range, and its value decreases with increasing temperature [8,9]. However, it has been demonstrated that for certain biological processes, Q_{10} remains relatively stable (i.e., invariant) over a range of temperatures [7,8]. Understanding the temperature dependence of biochemical reactions and their interactions is fundamental to linking changes at the molecular level to higher levels of biological organization. Even with simple biochemical pathways and the absence of allosteric regulation, it has previously been shown that the pathway Q_{10} cannot be inferred from the temperature dependencies of isolated reactions within the pathway [10]. Metabolic modeling can be employed to predict fluxes of the entire network at different temperatures to bridge the gap between individual reactions and the whole metabolic network.

We previously integrated targeted time-course metabolomics data with a cell-scale metabolic model [14,15] to characterize the temperature dependence of the human red blood cell (RBC) metabolic network [7]. RBCs are an advantageous system to study due to the relatively small size of the metabolic network, lack of organelles, and lack of transcriptional and translational regulation. Human platelets (PLTs) lack a nucleus but contain mRNAs and the protein machinery necessary for de novo protein synthesis [16]; however, the basal protein synthesis in PLTs is low and is mainly linked to signal-dependent activation [16,17]. Therefore, temperature-dependent metabolic changes in resting PLTs are therefore unlikely to be heavily influenced by genomic regulation. While RBCs rely entirely on glycolysis for energy generation, PLTs contain mitochondria and depend on oxidative phosphorylation to generate energy [18]. Thus, the human PLT represents a good human cell model to study the network-level temperature dependence of oxidative cellular metabolism.

PLTs stored in a blood bank setting represent a practical context for studying the temperature dependence of metabolism. Platelet concentrates (PCs) are used in modern medicine to reduce the risk of bleeding or control active bleeding in patients [19]. Under current blood banking practices, PCs are stored in gas-permeable plastic bags at 22 °C under constant agitation. Storing platelets at such a high temperature limits the shelf life to 5–7 days (depending on the country), mainly due to the risk of bacterial infection and the deterioration of PLT quality during storage (the “platelet storage lesion” (PSL) [20]). Storing PCs at lower temperatures provides increased storage time and a reduced risk of bacterial infection. However, as first demonstrated by Murphy and Gardner in 1969, PLTs stored at 4 °C show reduced post-transfusion survival compared with platelets stored at room temperature [21,22]. Nonetheless, there is a growing interest in using cold-stored PLTs to control bleeding in trauma patients due to superior hemostatic function and the immediate rather than long-term needs of those patients [23–25].

The metabolism of stored PLTs has been extensively studied [18,26–31]. Recently, we conducted a systems analysis of PLT metabolism during storage in platelet additive solution (PAS) [31] using a modified version of a previously published PLT metabolic network reconstruction [32]. During storage, PLTs can utilize a variety of nutrients [18] and rely on both glycolytic and oxidative metabolic pathways for energy production [26,31]. The temperature effects on platelet metabolism have mostly been investigated in the context of the glycolytic activity of PCs stored at 4 °C by measuring the decreased uptake and secretion rates of glucose and lactate, respectively [33–35]. More recently, multiomic approaches have confirmed these findings and highlighted a decreased energy demand of PCs during cold storage accompanied by reduced oxidative stress [36,37]. A formal quantitative study on the effects of temperature on the metabolic network has not yet been conducted.

Here, we used targeted time-course metabolomics analysis of stored PCs to assess the PLT metabolic network at four different temperatures (4 °C, 13 °C, 22 °C, and 37 °C). We integrated these data into a cell-scale computational model of PLT metabolism [15,31] to predict the metabolic flux of the entire metabolic network. The resulting data-driven model

allows for the estimation of Q_{10} values for individual metabolic reactions and pathways comparison of network-level responses to temperature changes.

2. Materials and Methods

2.1. Preparation and Storage of PCs

Buffy-coat pools were obtained from 8 healthy donors at the Blood Bank at Landspítali-University Hospital, Iceland. Four leukoreduced buffy-coat pools were combined and then split into four identical PCs containing approximately 65% platelet additive solution (SSP+, MacoPharma, Tourcoing, France) and 35% plasma. The PCs were stored in plastic containers (PL 2410, Lake Zurich, Fenwal, IL, USA) under constant agitation at four different temperatures: 4 °C, 13 °C, 22 °C, and 37 °C. The National Bioethics Committee of Iceland approved the study.

2.2. Sample Collection

The samples were collected at seven different time points from each PC. From the PC stored at 4 °C, samples were collected at 24 h, 48 h, 108 h, 216 h, 324 h, 432 h, and 552 h; from the PC stored at 13 °C, samples were collected at 24 h, 48 h, 60 h, 120 h, 180 h, 240 h, and 312 h; from the PC stored at 22 °C, samples were collected at 24 h, 48 h, 72 h, 96 h, 120 h, 144 h, and 168 h. From the PC stored at 37 °C, samples were collected at 3 h, 6 h, 24 h, 27 h, 30 h, 48 h, and 51 h. Sample collection procedures were conducted as previously reported [29].

2.3. Assays

Immediately after sample collection, PC quality assessment was performed using a hematology analyzer (CELL-DYN Ruby, Abbott Diagnostics, Abbott Park, IL, USA) to measure hematological parameters, and a blood gas analyzer (ABL90 FLEX, Radiometer Medical ApS, Brønshøj, Denmark) to measure the concentrations of glucose, lactate, pH, and ion concentrations. The quality assessment results can be found in Supplementary File S1 (Tables S1 and S2). The extracellular acetate concentration was measured with an enzymatic coupled assay (ACETAK), according to the manufacturer's instruction (Megazyme International Ireland Ltd., Wicklow, Ireland), using a microplate reader (Spectramax M3, Molecular Devices, Sunnyvale, CA, USA).

2.4. Metabolomics

The metabolomics analysis follows the same procedure as explained in [29]. Briefly, samples were split into extra- and intracellular fractions by centrifugation. Polar metabolites were extracted using cold methanol:water extraction (7:3) followed by evaporation and resuspension in acetonitrile:water (1:1). The metabolites were separated and detected using ultra-performance liquid chromatography (UPLC; Acquity, Manchester, UK) coupled to a quadrupole time-of-flight mass spectrometer (Q-TOF MS; Synapt G2, Waters, Manchester, UK). Chromatographic separation was achieved by hydrophilic interaction liquid chromatography (HILIC) using two conditions: (1) Acidic mobile phase (ACN:water with 0.01% formic acid) measured in both positive and negative ionization modes. (2) Basic mobile phase (ACN:water with 10 mM ammonium bicarbonate) measured in negative ionization mode. A calibration mixture of 72 metabolites was measured at eight concentrations within each batch. All samples were measured in triplicates in a randomized order. The metabolites were identified by matching chromatographic retention times and mass-to-charge ratios to our in-house database. Targetlynx (v4.1, Waters, Manchester, UK) was used to integrate the chromatographic peaks. The integrated peaks were normalized to appropriate internal standards for the relative quantification of targeted metabolites. Absolute quantification of selected metabolites was carried out by using standard curves generated by the calibration mixture. Principal component analysis (PCA) was performed using R v3.5.1 (R Development Core Team, Vienna, Austria). Prior to running the PCA

algorithm, the data were normalized using z-scores. Hierarchical clustering and heatmap generation were performed using MetaboAnalyst v.3 [38].

2.5. Temperature Coefficient Q_{10} Calculation

The Q_{10} coefficient describes the ratio of rates between temperatures differing by 10 °C. The Q_{10} is given by:

$$Q_{10} = \left(\frac{k_2}{k_1} \right)^{\frac{10}{T_2 - T_1}}$$

where T_1 and T_2 are temperatures in Kelvin (with $T_2 > T_1$), and k_1 and k_2 are the rates at T_1 and T_2 , respectively. In cases where Q_{10} is relatively temperature invariant, a regression line can be fitted to the logarithm of the reaction rates against temperature according to

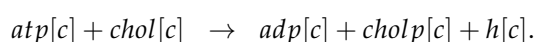
$$\ln Q_{10} = 10 \cdot \frac{\ln k_2 - \ln k_1}{T_2 - T_1} = 10 \cdot m$$

where the slope of the regression line m can then be used to estimate Q_{10} through

$$Q_{10} = e^{10 \cdot m}.$$

2.6. Constraint-Based Metabolic Modeling

To estimate the flux states at each temperature, we used a modified version of the platelet metabolic reconstruction iAT-PLT-636 [32] following the same procedures as in [31]. This modified version was previously used for metabolic network analysis of buffy coat and apheresis-derived PCs stored in PAS [31]. Here, further modifications have been made to accommodate choline metabolism by adding the choline kinase reaction (CHOLK):



This reaction can be catalyzed by the choline/ethanolamine kinase *CHKB*, which has been detected in platelets through proteomic analysis [31]. A linear regression line was fitted to the time-concentration profile of all extracellular metabolites used as model constraints at each temperature.

The slopes of the regression lines, normalized to the average platelet count at each condition, were used to estimate the uptake/secretion rate of the selected metabolites, similar to previous studies. The slopes of the regression lines, normalized to the average platelet count at each condition, were used to estimate the uptake/secretion rate of the selected metabolites, similar to previous studies [15]. In the case of infeasible models, an optimization algorithm was used to slightly adjust the constraints to obtain a feasible solution, as described in [31]. For each constrained model, random sampling of the solution space [39] was carried out 5000 times. The model analysis was conducted in MATLAB (Mathworks, Natick, MA, USA) using the COBRA Toolbox [40].

3. Results

3.1. Metabolite Time–Concentration Profiles Scale Non-Uniformly with Temperature

We analyzed both the extra- and intracellular metabolites in stored PCs. A total of 62 metabolites were measured in the extracellular fractions and 72 metabolites in the intracellular fractions. Underlying trends in the metabolomics data were analyzed by PCA [41] to identify how the metabolome scales with temperature. We observed a clear separation in both the extra- and intracellular metabolic profiles of the PCs stored at different temperatures (Figure 1). Notably, we observed that the largest variance was due to storage time in the extracellular fraction (Figure 1a) but storage temperature in the intracellular fraction, with increasing separation as storage time increased (Figure 1b).

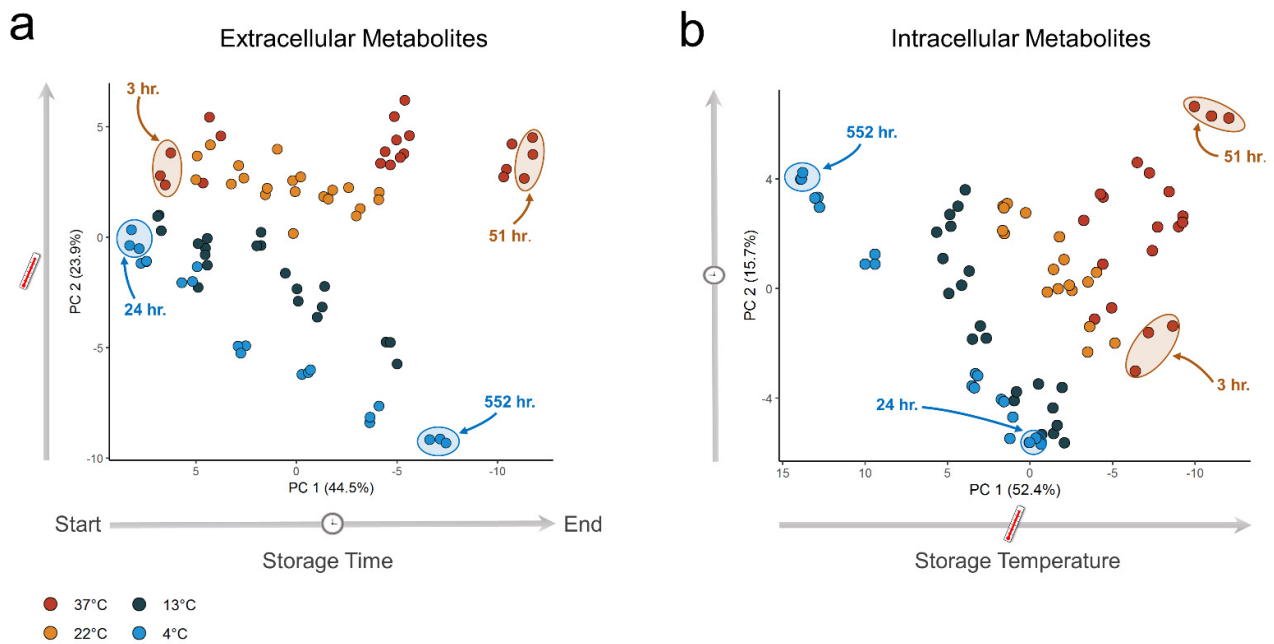


Figure 1. Principal component analysis (PCA) of extra- and intracellular metabolite data. Samples were collected at seven time points at four different temperatures—all samples were measured in triplicates. (a) PCA score plot for the extracellular fractions. (b) PCA score plot for the intracellular fractions.

The extra- and intracellular metabolic profiles were analyzed by hierarchical clustering with a heatmap to visualize the time-dependent effects temperature has on the metabolome. In the extracellular fractions, distinct groups of metabolites were observed (Figure 2). One group of metabolites increased in concentration with storage time at all temperatures with rates proportional to temperature, including phenylalanine and xanthine. Another group—including cysteinylglycine disulfide and cysteineglutathione disulfide—decreased in concentration with rates inversely proportional to temperature (i.e., the rate of formation and breakdown of a subset of the extracellular metabolome increased with increased temperature). However, this trend was not observed for all measured metabolites; for example, the concentrations of aspartate and taurine increased with storage time at rates inversely proportional to temperature, while some metabolites were only secreted at 37 °C (e.g., sphingosine 1-phosphate (S1P) and acetylcarnitine).

In the intracellular fractions (Figure 3), we observed higher concentrations of most measured metabolites at higher temperatures. A large fraction of the metabolome increased with the highest rate in the 37 °C PLTs, including many intermediates of phosphatidylcholine degradation (e.g., lysophosphatidylcholines (LysoPCs) and choline). Conversely, a group of metabolites—including glutathione and S1P—were maintained at higher concentrations at 4 °C compared to the other temperatures. In the PLTs stored at 4 °C, there was a noticeable drop in concentration for most of the measured metabolites at 24 h, with the notable exception of adenine and adenosine. These metabolites increased sharply in concentration at the same time point, coinciding with the depletion of extracellular glucose. These results demonstrate that the temperature dependence of the metabolome of stored PLTs is complex; that is, the reaction rates do not uniformly increase with increased temperature.

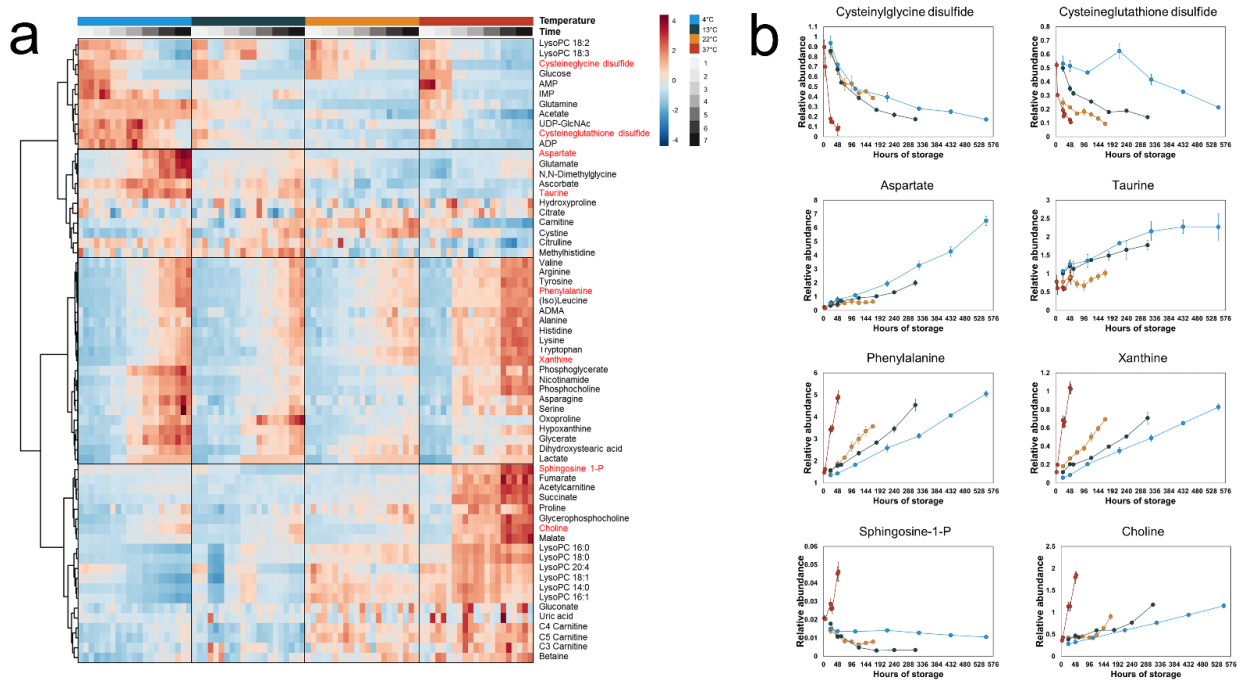


Figure 2. Time-concentration profiles of the extracellular metabolites. (a) A heatmap of all measured extracellular metabolites. Hierarchical clustering grouped the metabolites into four distinct clusters. (b) Line plots of selected metabolites representative of each cluster. The points represent the mean of the normalized metabolite abundance and the error bars standard deviation.

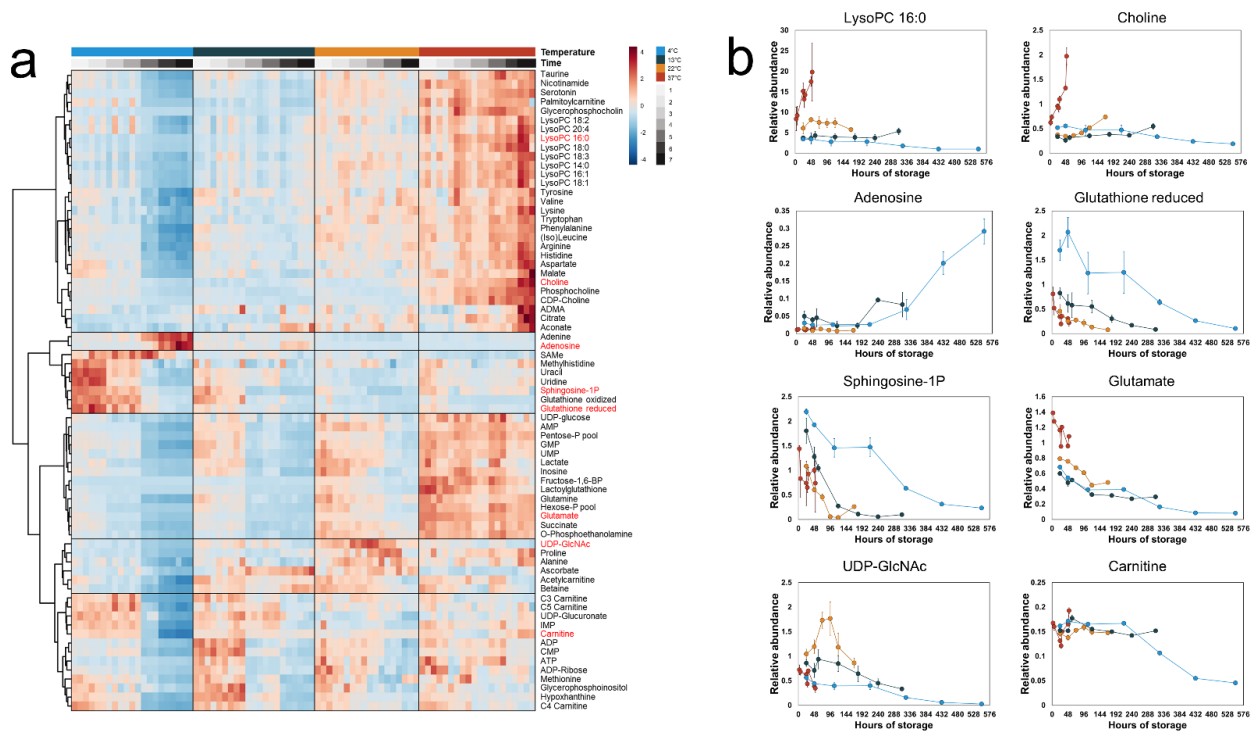


Figure 3. Time-concentration profiles of the intracellular metabolites. (a) A heatmap of all measured intracellular metabolites. Hierarchical clustering grouped the metabolites into six distinct clusters. (b) Line plots of selected metabolites representative of each cluster. The points represent the mean of the normalized metabolite abundance and the error bars standard deviation.

3.2. A Subset of Extracellular Metabolites Follows an Arrhenius-Type Relationship with Temperature

The data summarized in Figure 1 demonstrate that platelet metabolism follows a temperature-specific trajectory, in contrast to what would be expected if the rate of change in the metabolome would simply scale uniformly with temperature. However, as observed in Figure 2, a subset of the metabolites did scale with temperature. The extracellular metabolites represent end nodes of the pathways that produce or consume them, acting as proxies for the temperature dependencies of those pathways.

To estimate Q_{10} for the rate of change in concentration of the extracellular metabolites, only metabolites where the concentrations varied linearly ($R^2 > 0.7$) with time during the entire storage time were selected. With this criterion, the concentrations of 19 metabolites were found to vary linearly with storage time, and their log-transformed rates varied linearly with temperature, with R^2 ranging from 0.80 to 0.99 (Table 1). This linearity allowed for a single Q_{10} estimation for the entire temperature range. The estimated Q_{10} values for the extracellular metabolites ranged from 1.54 to 3.04 with a median of 2.15 (Table 1), a finding in good agreement with the expected range of 2–3 for in vitro biological reactions [7].

Table 1. Q_{10} coefficient for extracellular metabolites.

Metabolite	Q_{10}	R^2
Alanine	2.37	0.99
Arginine	2.02	0.92
Cysteineglycine disulfide	2.14	0.94
Glucose	1.73	0.99
Glycerate	1.54	0.89
Histidine	2.30	0.98
Hypoxanthine	1.77	0.84
(Iso)Leucine	2.04	0.95
Lactate	1.70	0.98
Lysine	2.25	0.94
Malate	3.04	0.93
Nicotinamide	2.01	0.83
Phenylalanine	2.05	0.94
Phosphocholine	2.16	0.80
sn-Glycero-3-phosphocholine	2.50	0.98
Tryptophan	2.15	0.96
Tyrosine	2.15	0.94
Valine	2.18	0.97
Xanthine	2.23	0.94

3.3. Acetate and Glutamine Metabolism Is More Sensitive to Temperature Than Glucose Metabolism

The most important fuels for ATP turnover in PCs stored in PAS at standard storing conditions (22 °C) are acetate, glucose, and glutamine [31]. The time–concentration profiles of these three metabolites and lactate increased at different rates with temperature (Figure 4). Acetate and glutamine uptake halted at 4 °C, while changes to glucose uptake and lactate secretion rates were less sensitive to temperature. The changes in uptake and secretion rates were quantified by estimating the respective Q_{10} coefficients. Since no detectable uptake of acetate was recorded at 4 °C, it was excluded from the Q_{10} calculation. Acetate uptake between temperatures 13–37 °C had a calculated $Q_{10} = 2.98$, which was relatively temperature invariant ($R^2 > 0.99$). Glutamine uptake (Figure 4) occurred at similar rates at 37 °C and 22 °C but decreased at 13 °C. Glutamine uptake did not display an Arrhenius-type relationship with temperature; therefore, the Q_{10} was not estimated. In all PCs, glucose was depleted during the recorded storage time; only time points with non-zero glucose concentration were used for the Q_{10} calculations for glucose uptake and lactate secretion. We observed lower Q_{10} values for glucose (1.73, $R^2 > 0.99$) and lactate (1.70, $R^2 = 0.98$) than for acetate, i.e., temperature had a lesser impact on glucose uptake and lactate secretion

than on acetate uptake. In PLTs, glucose is primarily metabolized via glycolysis while acetate and glutamine fuel the TCA cycle. These results reflect an altered scaling of the two main energy-producing pathways in stored platelets with temperature. Interestingly, the relative contribution of these two pathways was reflected in the pH of the stored PCs. Acetate catabolism removes a proton from the extracellular environment whereas glycolytic breakdown of glucose results in the production of protons that are co-transported with lactate out of the cells. Correspondingly, the pH decreased slightly in the PC unit stored at 4 °C, while the pH increased in the PCs stored at higher temperatures, especially after glucose was depleted (Supplementary Figure S1). In all units, the pH remained above the recommended threshold set by the European Directorate for the Quality of Medicines & HealthCare [42].

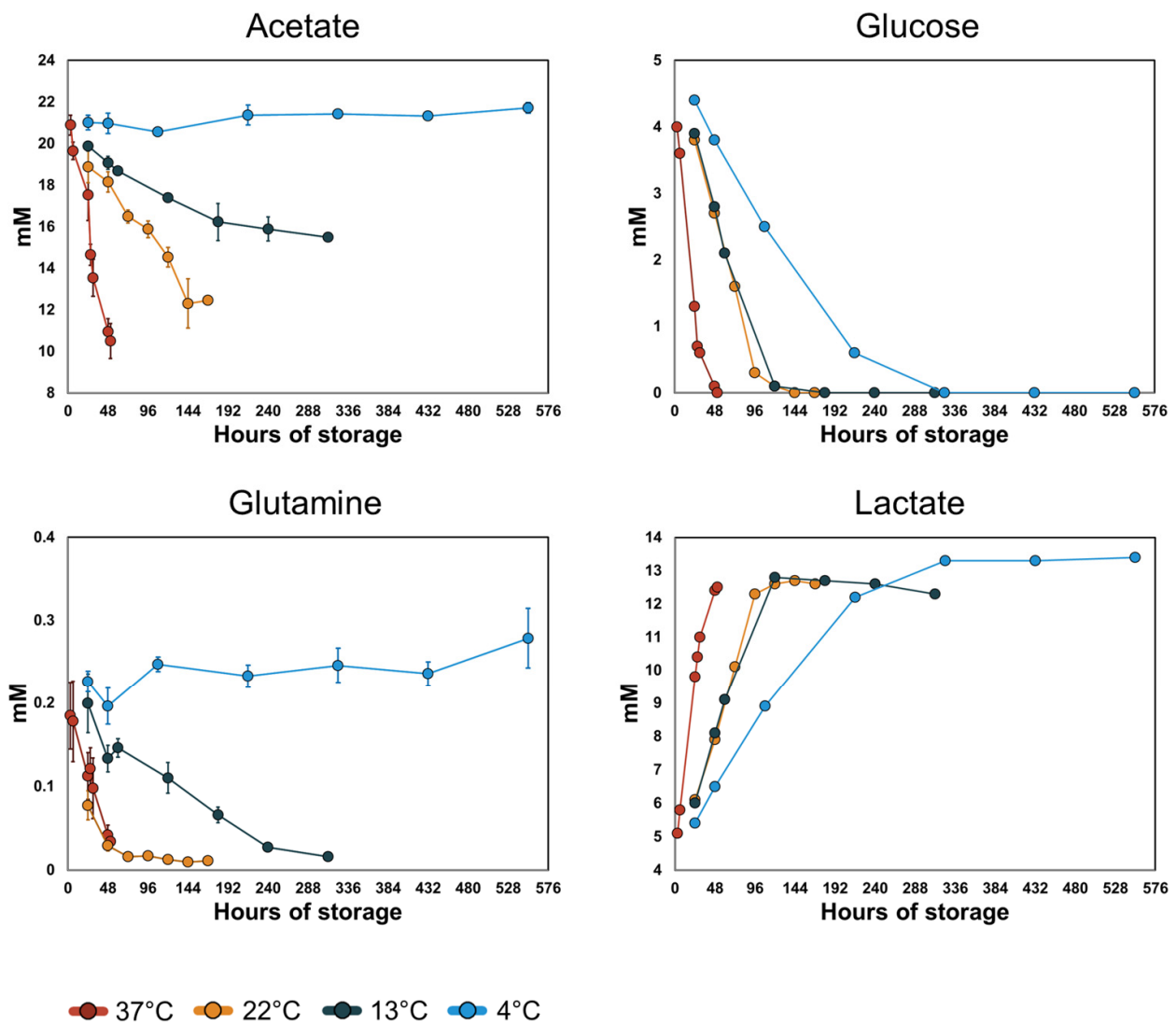


Figure 4. Time–concentration profiles of the main energy producing metabolites and lactate. The points represent the means of the measured values and the error bars the standard deviation. The rates of uptake of acetate and glutamine increase with increasing temperature with no detected uptake at 4 °C. The rates of glucose uptake and lactate secretion increase with increasing temperature. In all PCs, glucose was depleted during the recorded storage time. Due to this behavior, only time points with non-zero concentrations of glucose and lactate were used for the Q_{10} calculations.

3.4. Metabolic Modeling Reveals Pathway-Specific Temperature Dependence

Next, we integrated the measured metabolomics data with a metabolic network reconstruction of the human PLT [31,32] to investigate the temperature dependence on the metabolic pathway level. Previous metabolomics studies on PLTs stored in PAS revealed discreet metabolic phenotypes over storage time, with a transition from the first to second phenotypes occurring on day 4 of storage [29,30]. For the metabolic modeling, only the first phenotype (days 1–3) was chosen because (i) the first phenotype represents relatively fresh PLTs that still have not gone through extensive PSL, and (ii) at this stage, the extracellular glucose had not been depleted, and its uptake rates were constant at the different temperatures.

Relative aging was assumed to follow an Arrhenius model to estimate the equivalent time period for the PCs stored at temperatures other than 22 °C. A Q_{10} of 2.0 was chosen to model this relationship, roughly corresponding to time points 3–24 h at temperature 37 °C, 24–72 h at 22 °C, 24–120 h at 13 °C, and 24–216 h at 4 °C. At these time points, glucose had not been depleted, and the rates of change in concentration vary linearly with time for glucose, lactate, and acetate (except at 4 °C).

The following criteria were used to estimate Q_{10} coefficients for individual reactions: the reaction must be active (i.e., rate $> 10^{-6}$ mmol/day/PLT·10¹²) at all temperatures, and the Q_{10} coefficient must be relatively temperature invariant ($R^2 > 0.7$). A total of 530 (after removing exchange and sink reactions) reactions were predicted to be active at all temperatures, of which 117 reactions had relatively temperature-independent Q_{10} coefficients with a median of 2.23 (1.72–3.65).

The 117 reactions were sorted into 10 subsystems (Table 2) as defined by the global human metabolic network reconstruction [43] to investigate the relative temperature sensitivity of distinct metabolic pathways. A notable difference in Q_{10} values was observed in the energy-producing subsystems: glycolysis, citric acid cycle, and oxidative phosphorylation. Specifically, the citric acid cycle and oxidative phosphorylation had higher Q_{10} values than the median of all the reactions, while the Q_{10} values for glycolysis were comparatively lower. The majority of reactions within these pathways had temperature invariant Q_{10} , with the notable exception of four out of 13 reactions that are categorized as part of the TCA cycle but are not mitochondrial (e.g., cytosolic ATP citrate lyase, cytosolic isocitrate dehydrogenase, etc.), and 5 out of 18 reactions categorized as being part of glycolysis but do not contribute significantly to ATP production (e.g., phosphoglucomutase, reactions of the 2,3-DPG shunt). Flux through these reactions was predicted to be almost non-existent compared to flux through central glycolysis and the TCA cycle, and was therefore not considered in the interpretation of energy metabolism (Supplementary Material S3).

Table 2. The distribution of predicted Q_{10} in different subsystems of the metabolic network. The table displays median values with minimal and maximal values in parenthesis. The “Number of reactions” column refers to the number of reactions within a subsystem that had a relatively temperature invariant Q_{10} , and the number in parenthesis denotes the total number of reactions within each subsystem.

Subsystem	Q_{10}	R^2	Number of Reactions
Alanine and aspartate metabolism	2.28 (1.97–2.80)	0.91 (0.90–0.93)	5 (5)
Citric acid cycle	2.58 (1.97–2.70)	0.97 (0.90–0.98)	9 (13)
Fatty acid oxidation	2.21 (2.22–2.55)	0.91 (0.76–0.98)	8 (16)
Glycerophospholipid metabolism	2.23 (2.14–2.33)	0.72 (0.71–0.95)	37 (101)
Glycolysis/gluconeogenesis	1.76 (1.72–1.77)	0.98 (0.96–0.99)	12 (18)
Inositol Phosphate metabolism	2.21 (2.21–2.22)	0.95 (0.93–0.96)	4 (124)
Nucleotide interconversion	2.26 (2.22–2.70)	0.97 (0.95–0.98)	4 (21)
Oxidative phosphorylation	2.46 (2.27–2.47)	0.98 (0.98–0.98)	5 (5)
Triacylglycerol synthesis	2.22 (2.21–2.25)	0.82 (0.73–0.90)	7 (43)
Other	2.27 (1.73–3.65)	0.95 (0.74–0.99)	26 (184)
Total	2.23 (1.72–3.65)	0.90 (0.71–0.99)	117 (530)

We visualized the metabolic flux in glycolysis and the TCA cycle relative to the glucose uptake rate at each temperature to understand better how metabolism evolves over the temperature range. These showed an apparent flux decrease in the TCA cycle that is not dependent upon the decreased glucose uptake rate at lowered temperature but rather the decreased oxidation of acetate (Figure 5).

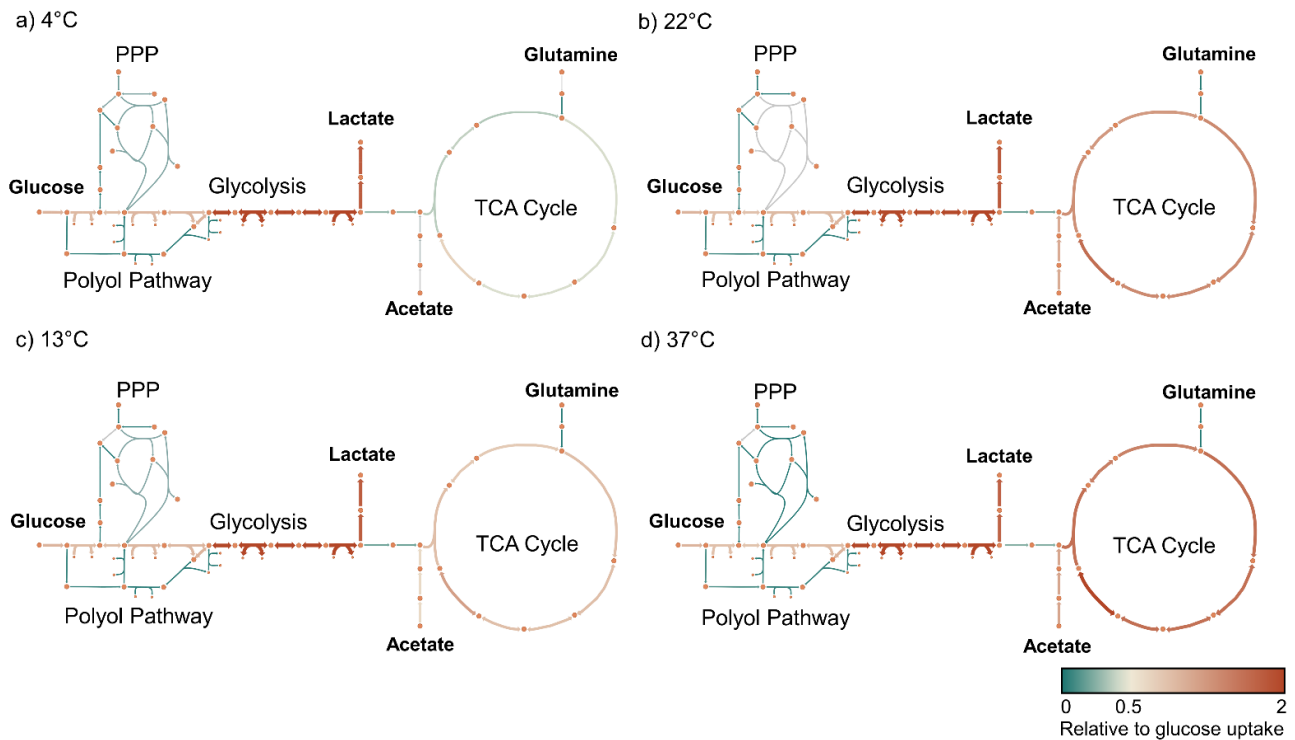


Figure 5. Metabolic flux within the TCA cycle decreases independently of the glucose uptake rate. Flux maps (a–d) showing the relative flux in $\text{mmol}(\text{gdw})^{-1}(\text{h})^{-1}$ normalized to the glucose uptake rate at each temperature. TCA cycle flux is diminished independently of glycolytic flux. We also visualized the absolute flux values through these pathways that showed a decrease in all the modelled reaction rates with decreasing temperature (Supplementary Figure S2).

Constraint-based modeling offers a framework for analyzing metabolism at the cellular level [14,44], allowing for quantitative predictions of cellular functions such as net ATP production and the relative contribution of the glycolytic and oxidative pathways to net ATP production [31]. Constraint-based models have previously been used to estimate the temperature dependence of a metabolic network [7], suggesting that the temperature dependence of these cellular processes could also be computed through the integration of metabolomics data [15]. The predicted Q_{10} for net ATP production was 2.24 ($R^2 > 0.99$). At all temperatures, oxidative metabolism was predicted to account for a higher proportion of ATP production. This proportion was, however, temperature dependent and increased with increasing temperature from 69.5% at 4 °C to 86.2% at 37 °C (Figure 6).

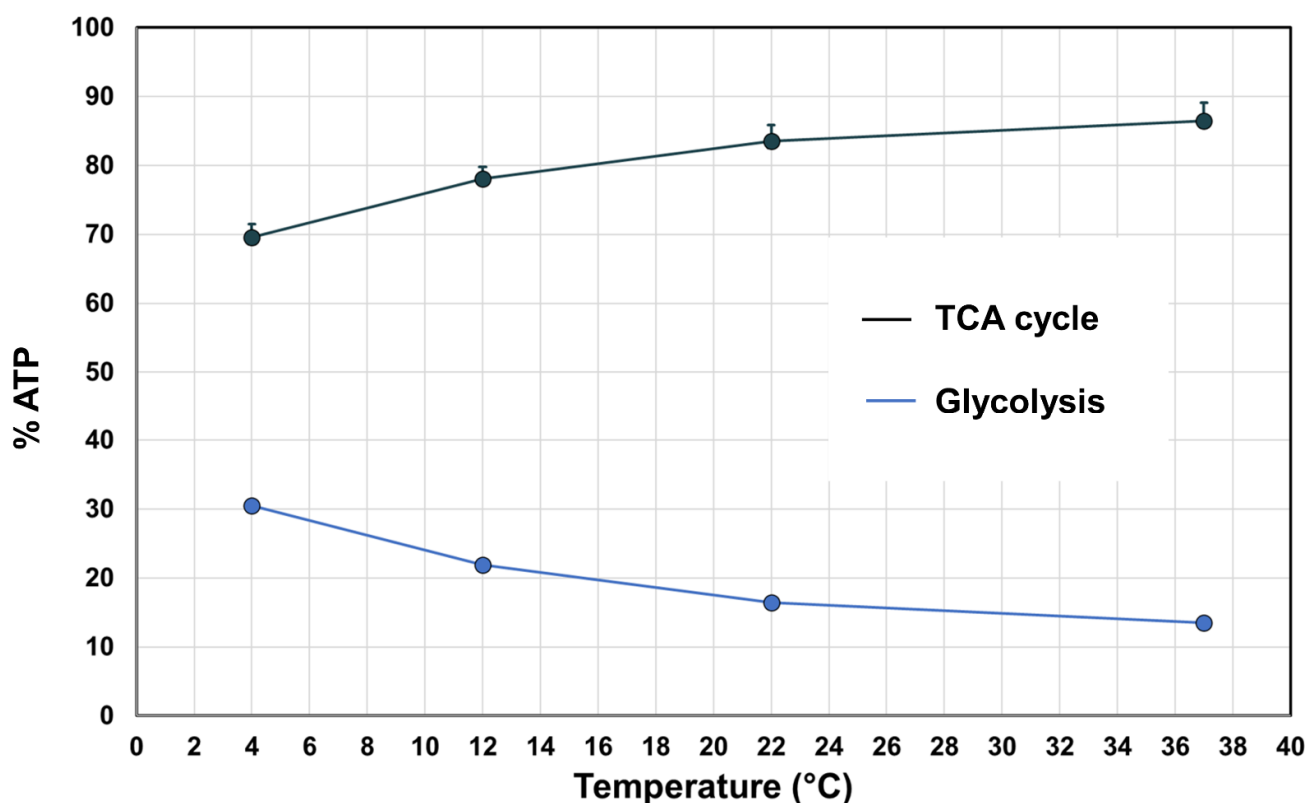


Figure 6. The relative contribution of glycolysis and oxidative metabolism to ATP production at different temperatures. The points represent the median of the random sampling results and the error bars the minimum and maximum.

4. Discussion

While it is well understood that temperature influences the rates of biological processes, the metabolic state of platelets stored at different temperatures has not been investigated. Here, we have investigated the temperature dependence of the PLT metabolic network during storage in PAS. We observed a non-uniform response over a 33 °C temperature range for 134 measured metabolites. This result is unsurprising since the metabolome represents the output of a complex system that depends on the kinetic properties of many enzymes, and many other factors, such as membrane fluidity, ionic strengths, and protein–protein interactions. Nonetheless, for a subset of the measured extracellular metabolites, the rate of change in concentration remained relatively constant throughout the storage time within each measured temperature. These rates could be modeled with an Arrhenius-type relationship to yield a single Q_{10} value over the entire temperature range. A global analysis of the metabolic network—using metabolomics data and computational models—indicated that pathway usage shifts as a function of temperature and is different depending upon the metabolic pathway.

Platelets are highly metabolically active cells [18] that utilize both glycolytic and oxidative metabolic pathways for energy production. Both processes are sensitive to temperature changes. The glycolytic activity can be assessed by measuring the glucose uptake rate and lactate secretion rate. The decrease in glycolytic activity at low temperatures reported here is in good agreement with previous studies comparing these parameters in PCs stored at 22 °C and 4 °C [33–37]. Between temperatures of 4 and 37 °C these rates, and as a proxy, the glycolytic rate, could be modeled by the Arrhenius equation with $Q_{10} \approx 1.7$, meaning that for every 10 °C increase in temperature, glycolytic activity increases 1.7-fold. In our prior analysis of red blood cells, the analogous Q_{10} was 2.8 [7].

Oxidative metabolism provides the bulk of ATP turnover in platelets [18,26,31]. In PCs stored in PAS at room temperature, acetate is the primary oxidative fuel and is mostly

converted to CO₂ via oxidative phosphorylation [28,31]. The Q_{10} coefficient for acetate uptake could not be estimated for the entire temperature range since no acetate uptake was detected at 4 °C. Acetate uptake was measured over the temperature range 13–37 °C, and a single value for the temperature coefficient could be obtained at $Q_{10} = 2.98$. These results indicate that the oxidative metabolism of stored PLTs is more sensitive to temperature changes than the glycolytic metabolism over the 4–37 °C range. Glutamine can be utilized as an oxidative fuel by platelets via glutaminolysis, which provides substrates for the TCA cycle [31,45]. The decrease in the uptake rate of glutamine at 13 °C and the absence of net uptake at 4 °C further indicate a slowdown of oxidative metabolism with decreasing temperature.

The PLT cell-scale model allows for predictions of flux distribution over the entire metabolic network given a set of constraints in the form of uptake/secretion rates. Here, we have utilized the PLT model to predict the flux state at four different temperatures by adding constraints of 20 extracellular metabolites measured at all temperatures. The results show that the Q_{10} values for stored PLTs fall within a relatively narrow range (1.72–3.65) compared to the previously computed flux states of stored RBCs [7]. Unsurprisingly, the overall metabolic rate decreased with decreasing temperature, consistent with previous reports showing increased intracellular ATP/AMP/ADP at lower temperatures [36,37]. The decrease in flux was not uniform, indicating that the relative fluxes through reactions and pathways change with temperature.

A representative example of this behavior can be seen in the lowered temperature sensitivity of glycolysis in platelets compared other pathways (Table 2). In our prior analysis of red blood cells, the analogous Q_{10} was 2.8 [7]. While initially, these data may indicate that glycolysis in platelets is less temperature sensitive than in red cells, flux through metabolic pathways is controlled by many factors, including the kinetic properties of the constituent enzymes, concentration of reactants and products, and activity of other pathways and cellular processes. In *E.coli*, for example, ATP-demanding processes have been shown to have the largest influence on the glycolytic flux [46]. In human PLTs, a decrease in oxidative metabolism either by inhibitors [45,47] or hypoxia [48] can be, at least partially, compensated for by increased glycolytic flux. Furthermore, platelet activation—an energy-demanding process—leads to increases in both glycolysis and oxidative metabolism [45,47], meaning that under basal conditions these pathways are maintained below their maximum capacity. It is, therefore, reasonable to assume that ATP demand is an important factor in the flux control of in PLTs, and that the thermal effects seen here on the PLT metabolic network are governed both by the temperature dependencies of the reactions within the pathways as well as the temperature dependencies of ATP-demanding processes. Thus, we hypothesize that the higher thermal sensitivity of oxidative metabolism leads to an upregulation in glycolysis and, consequently, that the glycolytic rate at lower temperatures is maintained closer to its maximum capacity, which would explain the relatively low Q_{10} of glycolysis compared to that of RBCs [7] and other pathways in the PLTs.

The observed shift from oxidative metabolism may be beneficial to PLT storage. PLTs stored at 4 °C have been demonstrated to have lower mitochondrial reactive oxygen species (ROS) levels, leading to a better preservation of mitochondrial function [49]. This observation could explain the glutathione levels at lower temperatures reported here (Figure 3b), which is consistent with previous reports [36,37]. One possible mechanism for this phenomenon is a decrease in flux through the complexes of the electron transport chain; however, the rate of mitochondrial ROS generation depends not only on the oxygen consumption rate but also on other factors such as the protonmotive force, the rate constant of O^{2•} production and the mitochondrial NADH/NAD⁺ ratio [50,51]. Ultimately, the data presented here are insufficient to provide a mechanistic link between temperature and ROS generation.

5. Conclusions

In this study, we have demonstrated that lowered temperature slows down oxidative phosphorylation more than glycolysis in stored PLTs. The fact that acetate and glutamine uptakes are halted at 4 °C raises the question of whether oxidative metabolism is at all active at low temperatures and the need for oxidative fuel in the additive solution in cold-stored platelets. Conversely, the relative contribution of glycolysis to energy production increases at lower temperatures, necessitating ample extracellular glucose concentration for long-term storage. Another factor to consider is the change in pH that occurs over the storage period. At lower temperatures, the pH decreases because of active glycolysis without the compensating effects of oxidative metabolism; in particular, acetate metabolism that removes protons from the extracellular environment. The results indicate that in order to store platelets at a lower temperature, an alternative buffer would be required to maintain pH above 6.4.

One limitation of the study is that no direct oxygen uptake measurements were made. The lack of experimental constraint on oxygen uptake in the models may introduce an over-estimation of oxidative phosphorylation at lower temperatures. Our results demonstrate that the response of the PLT metabolic network to temperature change is complex and causes shifts in relative pathway activity, most notably a shift from oxidative to glycolytic metabolism at lower temperatures.

Supplementary Materials: The following supporting information can be downloaded at: <https://www.mdpi.com/article/10.3390/metabo14020091/s1>, Table S1. Platelet concentrate quality control analysis measured with a blood gas analyzer, Table S2. Platelet concentrate quality control analysis measured with a hematology analyzer, Figure S1. Platelet concentrate pH measured with a blood gas analyzer, Figure S2. Metabolic flux within the TCA cycle decreases independently of the glucose uptake rate.

Author Contributions: Conceptualization, Ó.R. and Ó.E.S.; methodology, F.J., S.G., Ó.E.S. and Ó.R.; formal analysis, F.J., Ó.E.S. and Ó.R.; resources, Ó.E.S. and Ó.R.; data curation, F.J., S.G. and J.T.Y.; writing—original draft preparation, F.J.; writing—review and editing, F.J., Ó.E.S., S.G., J.T.Y. and Ó.R.; supervision, Ó.E.S. and Ó.R.; project administration, Ó.R.; funding acquisition, Ó.R., Ó.E.S. and F.J. All authors have read and agreed to the published version of the manuscript.

Funding: Landspítali University Hospital Research Fund #A-2018-058, and a University of Iceland PhD grant, 2017.

Institutional Review Board Statement: The study was conducted according to the guidelines of the Declaration of Helsinki and approved by the National Bioethics Committee of Iceland.

Informed Consent Statement: Not applicable.

Data Availability Statement: The data presented in this study are available in article or Supplementary Material.

Acknowledgments: The authors would like to express thanks to the staff at the Icelandic Blood Bank.

Conflicts of Interest: The authors declare no conflicts of interest.

References

1. Arrhenius, S. Über die Reaktionsgeschwindigkeit bei der Inversion von Rohrzucker durch Säuren. *Z. Für Phys. Chem.* **1889**, *4*, 226. [[CrossRef](#)]
2. Laidler, K.J. Unconventional applications of the Arrhenius law. *J. Chem. Educ.* **1972**, *49*, 343. [[CrossRef](#)]
3. Stein, R.B.; Gordon, T.; Shriver, J. Temperature dependence of mammalian muscle contractions and ATPase activities. *Biophys. J.* **1982**, *40*, 97–107. [[CrossRef](#)] [[PubMed](#)]
4. Anderson, G.; Scott, M. Determination of product shelf life and activation energy for five drugs of abuse. *Clin. Chem.* **1991**, *37*, 398–402. [[CrossRef](#)] [[PubMed](#)]
5. Jorjani, P.; Ozturk, S.S. Effects of cell density and temperature on oxygen consumption rate for different mammalian cell lines. *Biotechnol. Bioeng.* **1999**, *64*, 349–356.

6. Giacomini, M.; Schulte, P.M.; Wood, C.M. Differential Effects of Temperature on Oxygen Consumption and Branchial Fluxes of Urea, Ammonia, and Water in the Dogfish Shark (*Squalus acanthias suckleyi*). *Physiol. Biochem. Zool. PBZ* **2017**, *90*, 627–637. [CrossRef]
7. Yurkovich, J.T.; Zielinski, D.C.; Yang, L.; Paglia, G.; Rolfsson, O.; Sigurjonsson, O.E.; Broddrick, J.T.; Bordbar, A.; Wichuk, K.; Brynjolfsson, S.; et al. Quantitative time-course metabolomics in human red blood cells reveal the temperature dependence of human metabolic networks. *J. Biol. Chem.* **2017**, *292*, 19556–19564. [CrossRef]
8. Hegarty, T.W. Temperature Coefficient (Q₁₀), Seed Germination and Other Biological Processes. *Nature* **1973**, *243*, 305–306. [CrossRef]
9. Cohen Stuart, C.P. A study of temperature-coefficients and van't Hoff's rule. *K. Ned. Akad. Van Wet. Proc. Ser. B Phys. Sci.* **1912**, *14*, 1159–1173.
10. Chaui-Berlinck, J.G.; Navas, C.A.; Monteiro, L.H.; Bicudo, J.E. Temperature effects on a whole metabolic reaction cannot be inferred from its components. *Proc. Biol. Sci.* **2004**, *271*, 1415–1419. [CrossRef]
11. Chaui-Berlinck, J.G.; Monteiro, L.H.; Navas, C.A.; Bicudo, J.E. Temperature effects on energy metabolism: A dynamic system analysis. *Proc. Biol. Sci.* **2002**, *269*, 15–19. [CrossRef]
12. Donhoffer, S. The regulation of energy metabolism and van't Hoff's rule in the homeotherm animal. *Helgol. Mar. Res.* **1966**, *14*, 541–558. [CrossRef]
13. Gillooly, J.F.; Brown, J.H.; West, G.B.; Savage, V.M.; Charnov, E.L. Effects of Size and Temperature on Metabolic Rate. *Science* **2001**, *293*, 2248–2251. [CrossRef] [PubMed]
14. Orth, J.D.; Thiele, I.; Palsson, B. What is flux balance analysis? *Nat. Biotechnol.* **2010**, *28*, 245–248. [CrossRef] [PubMed]
15. Bordbar, A.; Yurkovich, J.T.; Paglia, G.; Rolfsson, O.; Sigurjonsson, Ó.E.; Palsson, B.O. Elucidating dynamic metabolic physiology through network integration of quantitative time-course metabolomics. *Sci. Rep.* **2017**, *7*, 46249. Available online: <https://www.nature.com/articles/srep46249#supplementary-information> (accessed on 12 December 2018). [CrossRef] [PubMed]
16. Schubert, P.; Devine, D.V. De novo protein synthesis in mature platelets: A consideration for transfusion medicine. *Vox Sang.* **2010**, *99*, 112–122. [CrossRef] [PubMed]
17. Zimmerman, G.A.; Weyrich, A.S. Signal-dependent protein synthesis by activated platelets: New pathways to altered phenotype and function. *Arterioscler. Thromb. Vasc. Biol.* **2008**, *28*, s17–s24. [CrossRef] [PubMed]
18. Guppy, M.; Whisson, M.E.; Sabaratnam, R.; Withers, P.; Brand, K. Alternative fuels for platelet storage: A metabolic study. *Vox Sang.* **1990**, *59*, 146–152. [CrossRef] [PubMed]
19. Kumar, A.; Mhaskar, R.; Grossman, B.J.; Kaufman, R.M.; Tobian, A.A.; Kleinman, S.; Gernsheimer, T.; Tinmouth, A.T.; Djulbegovic, B. Platelet transfusion: A systematic review of the clinical evidence. *Transfusion* **2015**, *55*, 1116–1127, quiz 1115. [CrossRef]
20. Devine, D.V.; Serrano, K. The platelet storage lesion. *Clin. Lab. Med.* **2010**, *30*, 475–487. [CrossRef]
21. Murphy, S.; Gardner, F.H. Effect of storage temperature on maintenance of platelet viability—Deleterious effect of refrigerated storage. *N. Engl. J. Med.* **1969**, *280*, 1094–1098. [CrossRef]
22. Marini, I.; Aurich, K.; Jouni, R.; Nowak-Harnau, S.; Hartwich, O.; Greinacher, A.; Thiele, T.; Bakchoul, T. Cold storage of platelets in additive solution: The impact of residual plasma in apheresis platelet concentrates. *Haematologica* **2019**, *104*, 207–214. [CrossRef]
23. Stubbs, J.R.; Tran, S.A.; Emery, R.L.; Hammel, S.A.; Haugen, D.A.L.; Zielinski, M.D.; Zietlow, S.P.; Jenkins, D. Cold platelets for trauma-associated bleeding: Regulatory approval, accreditation approval, and practice implementation—Just the “tip of the iceberg”. *Transfusion* **2017**, *57*, 2836–2844. [CrossRef]
24. Wood, B.; Johnson, L.; Hyland, R.A.; Marks, D.C. Maximising platelet availability by delaying cold storage. *Vox Sang.* **2018**, *113*, 403–411. [CrossRef] [PubMed]
25. Zhao, H.; Devine, D.V. The Missing Pieces to the Cold-Stored Platelet Puzzle. *Int. J. Mol. Sci.* **2022**, *23*, 1100. [CrossRef] [PubMed]
26. Kilkson, H.; Holme, S.; Murphy, S. Platelet metabolism during storage of platelet concentrates at 22 degrees C. *Blood* **1984**, *64*, 406–414. [CrossRef]
27. Murphy, S.; Shimizu, T.; Miripol, J. Platelet storage for transfusion in synthetic media: Further optimization of ingredients and definition of their roles. *Blood* **1995**, *86*, 3951–3960. [CrossRef]
28. Murphy, S. The oxidation of exogenously added organic anions by platelets facilitates maintenance of pH during their storage for transfusion at 22 degrees C. *Blood* **1995**, *85*, 1929–1935. [CrossRef]
29. Paglia, G.; Sigurjonsson, O.E.; Rolfsson, O.; Valgeirsdottir, S.; Hansen, M.B.; Brynjolfsson, S.; Gudmundsson, S.; Palsson, B.O. Comprehensive metabolomic study of platelets reveals the expression of discrete metabolic phenotypes during storage. *Transfusion* **2014**, *54*, 2911–2923. [CrossRef] [PubMed]
30. Paglia, G.; Sigurjonsson, O.E.; Rolfsson, O.; Hansen, M.B.; Brynjolfsson, S.; Gudmundsson, S.; Palsson, B.O. Metabolomic analysis of platelets during storage: A comparison between apheresis- and buffy coat-derived platelet concentrates. *Transfusion* **2015**, *55*, 301–313. [CrossRef]
31. Johannsson, F.; Gudmundsson, S.; Paglia, G.; Gudmundsson, S.; Palsson, B.; Sigurjonsson, O.E.; Rolfsson, O. Systems analysis of metabolism in platelet concentrates during storage in platelet additive solution. *Biochem. J.* **2018**, *475*, 2225–2240. [CrossRef] [PubMed]
32. Thomas, A.; Rahmanian, S.; Bordbar, A.; Palsson, B.O.; Jamshidi, N. Network reconstruction of platelet metabolism identifies metabolic signature for aspirin resistance. *Sci. Rep.* **2014**, *4*, 3925. [CrossRef] [PubMed]

33. Sandgren, P.; Shanwell, A.; Gulliksson, H. Storage of buffy coat-derived platelets in additive solutions: In vitro effects of storage at 4 degrees C. *Transfusion* **2006**, *46*, 828–834. [[CrossRef](#)] [[PubMed](#)]
34. NasrEldin, E. Effect of cold storage on platelets quality stored in a small containers: Implications for pediatric transfusion. *Pediatr. Hematol. Oncol. J.* **2017**, *2*, 29–34. [[CrossRef](#)]
35. Johnson, L.; Tan, S.; Wood, B.; Davis, A.; Marks, D.C. Refrigeration and cryopreservation of platelets differentially affect platelet metabolism and function: A comparison with conventional platelet storage conditions. *Transfusion* **2016**, *56*, 1807–1818. [[CrossRef](#)] [[PubMed](#)]
36. Zhao, H.W.; Serrano, K.; Stefanoni, D.; D’Alessandro, A.; Devine, D.V. In Vitro Characterization and Metabolomic Analysis of Cold-Stored Platelets. *J. Proteome Res.* **2021**, *20*, 2251–2265. [[CrossRef](#)] [[PubMed](#)]
37. D’Alessandro, A.; Thomas, K.A.; Stefanoni, D.; Gamboni, F.; Shea, S.M.; Reisz, J.A.; Spinella, P.C. Metabolic phenotypes of standard and cold-stored platelets. *Transfusion* **2020**, *60* (Suppl. S3), S96–S106. [[CrossRef](#)] [[PubMed](#)]
38. Xia, J.; Wishart, D.S. Using MetaboAnalyst 3.0 for Comprehensive Metabolomics Data Analysis. *Curr. Protoc. Bioinform.* **2016**, *55*, 14.10.1–14.10.91. [[CrossRef](#)]
39. Schellenberger, J.; Palsson, B.O. Use of randomized sampling for analysis of metabolic networks. *J. Biol. Chem.* **2009**, *284*, 5457–5461. [[CrossRef](#)]
40. Heirendt, L.; Arreckx, S.; Pfau, T.; Mendoza, S.N.; Richelle, A.; Heinken, A.; Haraldsdóttir, H.S.; Wachowiak, J.; Keating, S.M.; Vlasov, V.; et al. Creation and analysis of biochemical constraint-based models using the COBRA Toolbox v.3.0. *Nat. Protoc.* **2019**, *14*, 639–702. [[CrossRef](#)]
41. Worley, B.; Powers, R. Multivariate Analysis in Metabolomics. *Curr. Metabolomics* **2013**, *1*, 92–107. [[CrossRef](#)]
42. European Directorate for the Quality of Medicines & HealthCare. *Guide to the Preparation, Use and Quality Assurance of Blood Components: Recommendation no. R (95) 15*; European Directorate for the Quality of Medicines & HealthCare: Strasbourg, France, 2020.
43. Thiele, I.; Swainston, N.; Fleming, R.M.T.; Hoppe, A.; Sahoo, S.; Aurich, M.K.; Haraldsdottir, H.; Mo, M.L.; Rolfsson, O.; Stobbe, M.D.; et al. A community-driven global reconstruction of human metabolism. *Nat. Biotechnol.* **2013**, *31*, 419. Available online: <https://www.nature.com/articles/nbt.2488#supplementary-information> (accessed on 20 December 2018). [[CrossRef](#)]
44. Bordbar, A.; Monk, J.M.; King, Z.A.; Palsson, B.O. Constraint-based models predict metabolic and associated cellular functions. *Nat. Rev. Genet.* **2014**, *15*, 107–120. [[CrossRef](#)]
45. Ravi, S.; Chacko, B.; Sawada, H.; Kramer, P.A.; Johnson, M.S.; Benavides, G.A.; O’Donnell, V.; Marques, M.B.; Darley-Usmar, V.M. Metabolic plasticity in resting and thrombin activated platelets. *PLoS ONE* **2015**, *10*, e0123597. [[CrossRef](#)]
46. Koebmann, B.J.; Westerhoff, H.V.; Snoep, J.L.; Nilsson, D.; Jensen, P.R. The glycolytic flux in *Escherichia coli* is controlled by the demand for ATP. *J. Bacteriol.* **2002**, *184*, 3909–3916. [[CrossRef](#)]
47. Aibibula, M.; Naseem, K.M.; Sturmey, R.G. Glucose metabolism and metabolic flexibility in blood platelets. *J. Thromb. Haemost. JTH* **2018**, *16*, 2300–2314. [[CrossRef](#)] [[PubMed](#)]
48. Guppy, M.; Abas, L.; Arthur, P.G.; Whisson, M.E. The Pasteur effect in human platelets: Implications for storage and metabolic control. *Br. J. Haematol.* **1995**, *91*, 752–757. [[CrossRef](#)] [[PubMed](#)]
49. Bynum, J.A.; Meledeo, M.A.; Getz, T.M.; Rodriguez, A.C.; Aden, J.K.; Cap, A.P.; Pidcoke, H.F. Bioenergetic profiling of platelet mitochondria during storage: 4 degrees C storage extends platelet mitochondrial function and viability. *Transfusion* **2016**, *56* (Suppl. S1), S76–S84. [[CrossRef](#)] [[PubMed](#)]
50. Murphy, M.P. How mitochondria produce reactive oxygen species. *Biochem. J.* **2009**, *417*, 1–13. [[CrossRef](#)] [[PubMed](#)]
51. Aledo, J.C. Life-history Constraints on the Mechanisms that Control the Rate of ROS Production. *Curr. Genom.* **2014**, *15*, 217–230. [[CrossRef](#)] [[PubMed](#)]

Disclaimer/Publisher’s Note: The statements, opinions and data contained in all publications are solely those of the individual author(s) and contributor(s) and not of MDPI and/or the editor(s). MDPI and/or the editor(s) disclaim responsibility for any injury to people or property resulting from any ideas, methods, instructions or products referred to in the content.